

## Structural evolution of metallic glasses during annealing through in-situ

### Synchrotron X-ray diffraction

E. Pineda<sup>1,3\*</sup>, F. Boneu<sup>2</sup>, P. Bruna<sup>2,4</sup>, T. Pradell<sup>1,4</sup>, A. Labrador<sup>5</sup>, D. Crespo<sup>2,3</sup>

<sup>1</sup>Departament de Física i Enginyeria Nuclear, ESAB, Universitat Politècnica de Catalunya, Avda. del Canal Olímpic 15, 08860 Castelldefels, Spain

<sup>2</sup>Departament de Física Aplicada, EPSC, Universitat Politècnica de Catalunya, Avda. del Canal Olímpic 15, 08860 Castelldefels, Spain

<sup>3</sup>Centre de Recerca de l'Aeronutica i de l'Espai & <sup>4</sup>Centre de Recerca en Nanoenginyeria, UPC

<sup>5</sup>LLS - BM16, ESRF, 38043-Grenoble, France

\*Corresponding author:  
Eloi Pineda  
[eloi.pineda@upc.edu](mailto:eloi.pineda@upc.edu)  
Tel. (34) 935 521 141  
Fax. (34) 935 521 001

### Abstract

In this work we study the structural evolution of Al and Fe based metallic glass compositions. The samples were obtained as ribbons by melt-spinning, their glass stability and crystallization were analyzed by calorimetry and dilatometry, structural changes were followed by in-situ synchrotron X-ray diffraction during annealing throughout glass transition and crystallization. The synchrotron results are compared with calorimetric and dilatometric measurements and the structural changes occurred during annealing are determined and described for each alloy.

*Keywords:* Amorphous materials / metallic glasses / X-ray diffraction.

*Pacs:* 61.05.C, 61.43.Dq, 64.70.pe

### Introduction

Metallic glasses are promising materials both for fundamental research on the glass transition and crystallization phenomena and for technological applications. The properties of these materials are largely affected by their metastable state; different fracture, magnetic or elastic behaviours are observed in the same material as a function of the relaxation of the glassy state or the extent of nanocrystallization. In this work we analyze the structural changes occurred in metallic glasses during annealing. The chosen compositions,  $\text{Al}_{90}\text{Fe}_5\text{Nd}_5$  and  $\text{Fe}_{89}\text{Zr}_7\text{B}_4$ , are known to have primary crystallization processes leading to partially crystallized nanostructures [1, 2]. The in-situ synchrotron diffraction experiments allow us to relate the observed macroscopic changes (calorimetric and dilatometric measurements) to microscopic changes in the local structure.

## **Experimental**

Amorphous metallic ribbons were produced by melt-spinning. Composition was assessed by Energy Dispersive X-ray Spectroscopy (EDS), Differential Scanning Calorimetry (DSC) and dilatometry were realized in a DSC-822 Mettler-Toledo and Q800 TA-instruments. In the dilatometric experiments the change in ribbon length was measured applying a preload of 0.01N and a heating rate of 5 K/min using a tension clamp. The X-ray measurements were performed with radiation energy of 15KeV at the BM16 line of the European Synchrotron Radiation Facility (ESRF). The ribbons were fixed into a Linkam hot stage, the diffracted intensity was collected each 5s during the annealing by a two-dimensional CCD detector in transmission geometry. From the diffracted intensity, the total intensity elastically scattered by the samples  $I(Q)$  is obtained subtracting background and applying absorption[3], multiple scattering, and inelastic Compton scattering corrections[4]. Normalization of the scattered intensity was performed by the Krogh-Moe-Norman method and the total structure factor  $S(Q)$  was obtained using the values of the atomic factors tabulated in ref. [5,6,7]. The reduced radial distribution function  $G(r)$  is obtained by Fourier transformation and then the atomic radial distribution function  $RDF(r)$  can be computed [3,8]. The hot-stage window aperture and the experimental setup limited the measurement of the diffracted intensity up to  $Q_{\text{max}}=8\text{\AA}^{-1}$ . This small range in  $Q$  is expected to broaden artificially the peaks of the obtained radial distributions [8].

## Results

$\text{Al}_{90}\text{Fe}_5\text{Nd}_5$  alloy presents primary crystallization of fcc-Al at  $T_{x1}=180^\circ\text{C}$  (measured by DSC at 10 K/min) and a second crystallization stage with precipitation of various intermetallic phases [1] at  $T_{x2}=343^\circ\text{C}$ . The signal of these crystallization processes in DSC and dilatometry is shown in figure 1. The inset in figure 1 shows the heat flow measured by DSC compared to the derivative of volume change measured by dilatometry, both thermal expansion and heat release measurements are similarly sensible. In the synchrotron measurements, diffraction spectra were collected through the whole heating treatment. Inset in figure 2 shows the collected intensity at three different temperatures corresponding to the initial room temperature glassy state, the partially crystallized state between  $T_{x1}$  and  $T_{x2}$  and the completely crystallized material after the second crystallization process.

The position of the first diffracted intensity maximum  $Q_1$  is inversely proportional to the mean inter-atomic spacing. Assuming a homogeneously distributed free volume content in the glassy phase, the change in specific volume can be calculated by

$$\left[ \frac{Q_1(T_0)}{Q_1(T)} \right]^3 = \frac{V(T)}{V(T_0)} \quad (1)$$

where  $V$  is the mean atomic volume and  $T_0$  is a temperature reference; in this work  $T_0$  is the initial temperature of the heating treatment. Figure 1 (symbols) shows the volume change computed using equation (1). Before primary crystallization the volume increases with a linear thermal expansion coefficient of  $\alpha_{\text{th}}=20.0 \times 10^{-6} \text{ K}^{-1}$ . The crystallization process is marked by a sudden change of the amorphous peak position due to the appearance of crystalline reflections. These changes appear in the diffracted intensities as rapid deformations of the main amorphous peak before any clear crystalline peak is detected. Comparison with direct dilatometric volume change measurements (blue line) is also given in figure 1.

Figure 2 shows the  $RDF(r)$  obtained at room temperature and at  $T=183^\circ\text{C}$ . Although the change in the main diffraction peak position at this temperature indicates that the crystallization process is already starting, no changes are appreciated in the atomic distribution function. The

position,  $r_1$ , and full width at half maximum (FWHM) of the first  $RDF(r)$  peak are found to be  $r_1=3.10\text{\AA}$ , FWHM=0.93\text{\AA} and  $r_1=3.11\text{\AA}$ , FWHM=0.97\text{\AA} respectively for room temperature and  $T=183^\circ\text{C}$ . This increase of  $r_1$  and FWHM is expected because of thermal expansion. The coordination number is computed from the area under the peak and it is obtained to be CN=11.8, in accordance with other measurements realized in similar Al-based amorphous alloys [9].

$\text{Fe}_{89}\text{Zr}_7\text{B}_4$  alloy devitrifies at  $T_{x1}=517^\circ\text{C}$  through precipitation of bcc-Fe particles [2], the corresponding DSC signal is given in inset b) of figure 3. Specific volume changes measured by dilatometry (blue line) and synchrotron X-ray diffraction (symbols) are also shown in figure 3. The two measurement methods give very similar results, this agreement supports the assumption of a homogeneously distributed free volume in metallic glasses as was demonstrated by Yavari et al. in ref. [10]. In both measurements deviation from a linear thermal expansion behaviour is observed above  $T=200^\circ\text{C}$ . This is interpreted as structural relaxation releasing excess free volume arrested during rapid quenching of the ribbons. This low temperature relaxation is not the usual glass relaxation preceding glass transition, in this case the amorphous phase continues stable after the relaxation process during approximately  $200^\circ\text{C}$  before any sign of glass transition or crystallization is detected. In addition to the results presented in this work, preliminary results of dynamic mechanical analysis confirm the presence of a two step softening process during the annealing of these ribbons. The large extent of free volume arrested during rapid quenching may be responsible of atomic mobility and relaxation at relatively low temperatures, after that the atomic mobility is again arrested until temperatures close to  $T_{x1}$ .

At  $T_g=510^\circ\text{C}$ , just below crystallization, a sudden change of volume expansion rate is detected only in the synchrotron data, this may be the signature of a glass transition very close to crystallization. Dilatometric measurements do not show such behaviour, however, at these temperatures the softening of the glassy ribbons (with thickness of  $25\mu\text{m}$ ) may result in deformation under the applied load, this deformation hiding the pure thermal expansion contribution. The radial distribution functions do not show significant changes in the amorphous atomic structure during annealing, see inset a) of figure 3. Coordination number is computed to

be CN=7.9, the first-peak position is  $r_1=2.80\text{\AA}$  at room temperature and  $r_1=2.82\text{\AA}$  above  $500^\circ\text{C}$ , while the FWHM increases from  $0.95\text{\AA}$  to  $1.00\text{\AA}$ .

## Conclusions

Metallic glass rapidly quenched ribbons are analysed by synchrotron X-ray diffraction during in-situ annealing processes. The analysis of the main diffraction peak position allows us to follow the structural changes occurred during the experiment and relate them to the response obtained in macroscopic measurements of volume change and calorimetry. The structure factors and the corresponding atomic radial distribution functions are obtained at any temperature during annealing. Although structural changes between glassy states are hardly detectable from the obtained total structure factors at different temperatures, the analysis of the main diffraction peak position allows us to determine differences in free volume content, structural relaxation and the onset of crystallization.

## Acknowledgements

The authors thank Dr. J. Molera from the Universitat de Girona for her help in DSC and dilatometer measurements. Work funded by CICYT, grant MAT2004-01214 and Generalitat de Catalunya, grants 2005SGR00535 and 2005SGR201.

## References

- [1] K.R. Cardoso, A. Garcia-Escorial, W.J. Botta, J. Non-Cryst. Solids 273 (2000) 266-270.
- [2] L. Malkinski, A. Slawska-Waniewska, Materials Science and Engineering A226-228 (1997) 716-720.
- [3] Y. Waseda, The Structure of Non-Crystalline Materials, McGraw-Hill, 1980.
- [4] H.H.M. Balyuzi, Acta Cryst. A31 (1975) 600.
- [5] D. Waasmaier, A. Kirfel, Acta Cryst. A51 (1995), 416-413
- [6] L. Kissel, B. Zhou, S. C. Roy, S. K.S. Gupta, R. H. Pratt, Acta Cryst. A51 (1995) 271-288

- [7] *DABAX A Dynamic Database for X-ray Applications*. B. Roux and M.S. del Rio, European Synchrotron Radiation Facility.
- [8] Th. Proffen, S.J.L. Billinge, T. Egami, D. Louca, *Z. Kristallogr.* 218 (2003) 132-143.
- [9] A. Inoue, *Progress in Materials Science* 43 (1998) 365-520.
- [10] A.R. Yavari, A. Le Moulec, A. Inoue, N. Nishiyama, N. Lupu, E. Matsubara, W.J. Botta, G. Vaughan, M. Di Michiel, A. Kvik, *Acta mater.* 53 (2005) 1611-1619.

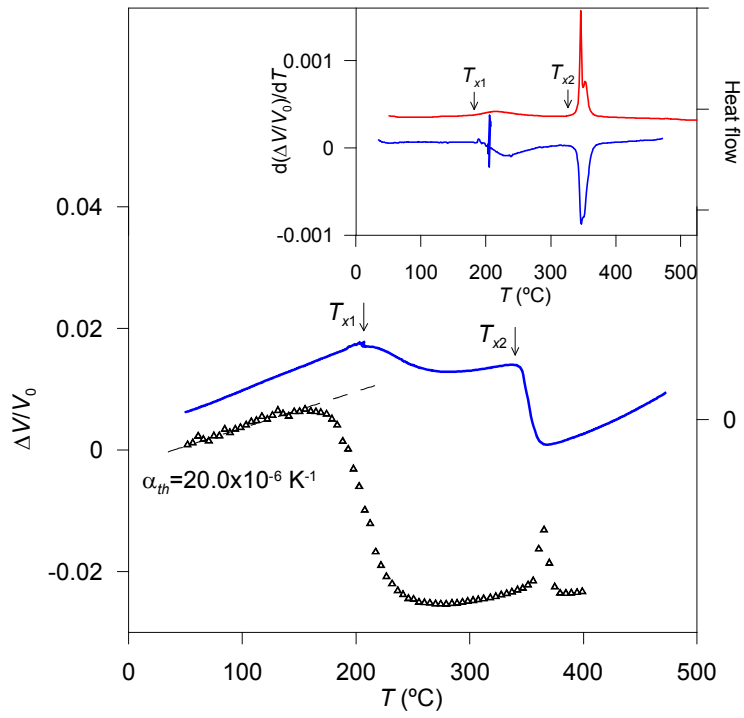


Figure 1.

Volume change measured by dilatometry at 5 K/min (blue line) and computed from the X-ray main diffraction peak position (symbols) of melt spun  $\text{Al}_{90}\text{Fe}_5\text{Nd}_5$  alloy. Inset: DSC signal at 10 K/min (red line) and derivative of volume change obtained from dilatometry at 5 K/min (blue line).

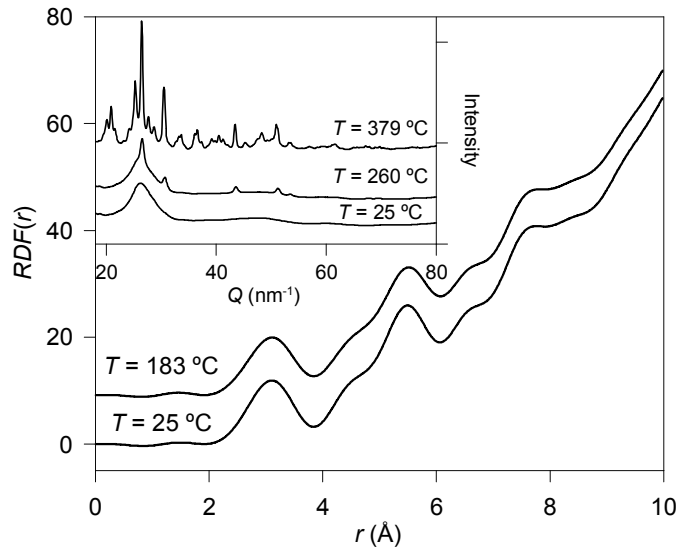


Figure 2.

Total atomic radial distribution function,  $RDF(r)$ , at two different temperatures for melt spun  $\text{Al}_{90}\text{Fe}_5\text{Nd}_5$  alloy. Inset: Diffracted intensity at three different temperatures during annealing.



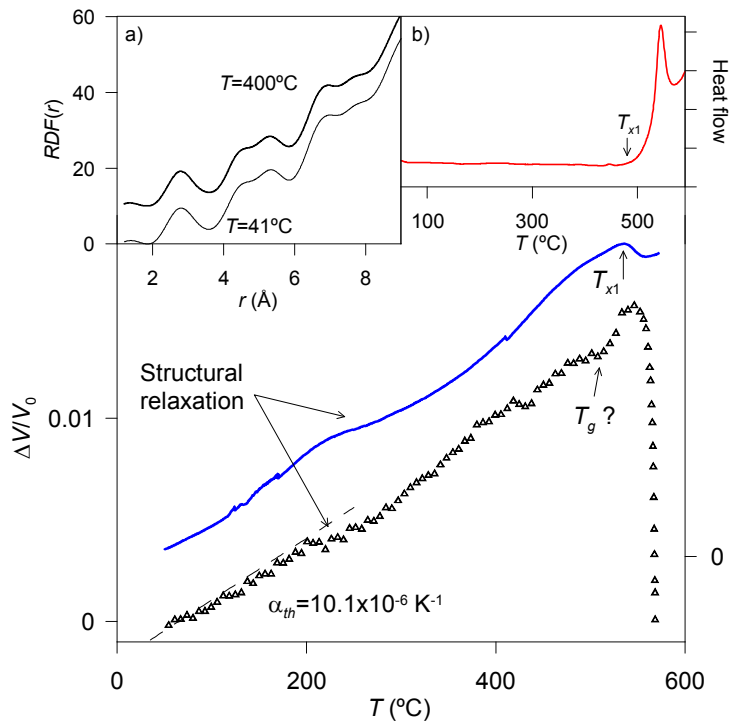


Figure 3.

Volume change measured by dilatometry at 5 K/min (blue line) and computed from the main X-ray diffraction peak position (symbols) of melt spun  $\text{Fe}_{89}\text{Zr}_7\text{B}_4$  alloy. Inset a): Total atomic radial distribution function at  $T=41^\circ\text{C}$ ,  $T=200^\circ\text{C}$  and  $T=400^\circ\text{C}$  during annealing at 20 K/min. Inset b): DSC signal at 10 K/min.